



Research Article

Potential of Cashew Leaf Extract for Mild Steel Corrosion Mitigation in Hydrochloric Acid Environment

Omotioma M., Onukwuli O. D, Obiora-Okafo I. A., Mbah G. O., Chime T. O., Udeh B. C., Agu Francis Anezichukwu, Onuora Okorie, Eketete J. A.

Special Issue

A Themed Issue in Honour of Professor Onukwuli Okechukwu Dominic (FAS).

This special issue is dedicated to Professor Onukwuli Okechukwu Dominic (FAS), marking his retirement and celebrating a remarkable career. His legacy of exemplary scholarship, mentorship, and commitment to advancing knowledge is commemorated in this collection of works.

Edited by
Chinonso Hubert Achebe PhD.
Christian Emeka Okafor PhD.

Potential of Cashew Leaf Extract for Mild Steel Corrosion Mitigation in Hydrochloric Acid Environment

Omotioma M.^{1*}, Onukwuli O. D.², Obiora-Okafo I. A.², Mbah G. O.¹, Chime T. O.¹, Udeh B. C.¹, Agu Francis Anezichukwu¹, Onuora Okorie¹, Eketete J. A.¹

¹Department of Chemical Engineering, Enugu State University of Science and Technology, P.M.B. 01660, Enugu, Nigeria

²Dept. of Chemical Engineering, Nnamdi Azikiwe University, P.M.B. 5025, Awka, Anambra State, Nigeria

*Corresponding Author's E-mail: omorchem@yahoo.com

Abstract

This study investigated cashew leaf's potential to reduce mild steel (MS) corrosion in an HCl environment. With the use of a gas chromatography-mass spectrophotometer, the molecular components of the extract were determined. The adsorption mechanism and characteristics of the corrosion inhibition process were determined using the gravimetric approach. Furthermore, artificial neural networks (ANN) and response surface methodology (RSM) were used to forecast the cashew leaf extract's inhibitory efficacy. According to the results, the main biomolecular components of the cashew leaf extract were 9-tetradecenal, oleic acid, 2-hydroxy cyclopenta decanone, 4H-pyran-4-one, 3,5-dihydroxy-6-methyl-2,3-dihydro-4H-pyran-4-one, 2-methyl-3-ketotetrahydrofuran, oxirane, 8-methyl-9-tetradecenoic acid, 2,3-butylene oxide, 2,3-dimethyloxirane and 3(2H)-furanone. The biomolecules spontaneously adhered to the MS surface, a physical adsorption event. The results of the optimization/prediction analyses demonstrated that when it came to forecasting the extract's efficacy, ANN outperformed RSM. The study's findings can serve as the basis for using cashew leaf as an additive to prevent mild steel from corroding in a corrosive environment.

Keywords: ANN, cashew leaf, corrosion, inhibition efficiency, RSM

1.0 Introduction

The need for scientists and engineers with technical expertise in corrosion control procedures has increased due to exigencies in industrial activity. These scenarios involve modifications to transportation and production methods that impact the dynamics of metal corrosion. Thus, new corrosion control data is needed for the deployment of novel materials for the production and delivery of useful products. Therefore, the goal of current research is to develop solutions for corrosion situations that are constantly changing. Researchers view the process of explaining the concept of corrosion as a respectable scientific endeavor. The term "corrosion" describes surface degradation or the deterioration of materials or metals in an unfriendly environment. When metal comes into touch with air, moisture, acidic solutions, or other corrosive environments, it oxidizes and degrades. There are two types of corrosion processes: chemical corrosion, which happens when a metal combines with oxygen or dry air, and electrochemical corrosion, which happens when an electrolyte is present. The tendency of metal to revert to its thermodynamically stable state is generally the main cause of metallic corrosion. That is, one of the features of metal corrosion is a decrease in a system's Gibbs energy (Bell et al, 2019). It has also been reported that corrosion results from an electrochemical reaction when metal is exposed to a corrosive environment (Xia et al, 2022). Reaction occurs when mild steel, which is high in iron, comes into touch with an acidic environment. For example, when HCl and iron combine, FeCl₂ and H₂ are produced:



Anodic and cathodic processes are two electrochemical phenomena that result from corrosion on a metal's surface. The equilibrium potential varies for each of these processes (Ushakov et al, 2021). Anodes and cathodes are two corrosion cells frequently used to illustrate charge transfer within metals and between metals and electrolytes (Kadhim et al, 2021). Cathodic or anodic reactions result from variations in the electron density at the attachment site. Electrons produced by the anode are consumed by the cathode during this process.

For corrosion control techniques to be used effectively, a thorough understanding of metals is necessary (Umoren et al, 2016; Millán-Ocampo et al, 2018; Anadebe et al, 2019; Mashuga et al, 2017). The corrosion control research must therefore take into account the basic idea of mild steel as a metal. One noteworthy material used in the transportation, building, and engineering sectors is mild steel (Omotioma, and Onukwuli, 2016). In a variety of media, especially acidic solutions, it is prone to corrosion. Due to its favorable properties, which include good tensile strength, ease of production, and the capacity to conduct heat and electricity, it is typically advised for industrial applications. Mild steel, one of the most often used materials in engineering and building projects worldwide, requires corrosion protection. So, to prolong the lifespan of MS constructions, different ways are implemented approaches to avoid corrosion and the rate at which it may spread. The negative effects of corrosion necessitate mitigation methods.

Some engineering constructions experience significant failures due to corrosion, such as the quick decay of metallic materials, which can be costly to repair. Because systems must be shut down during maintenance, time is wasted. Additionally, rust is harmful and can cause staff members to be injured. Thus, engineers and scientists worldwide have been encouraged to view corrosion as a severe issue that needs to be addressed right away (Yadav et al, 2016; Rodriguez-Clemente et al, 2018; Amodu et al, 2022). In this regard the use of inhibitors is found to be a prominent technique that is frequently used to mitigate corrosion (Salleh et al, 2021). There are various available inhibitors, but plant extract is preferred over other inhibitor candidates (drug, ionic liquid and polymeric substance) due to its availability, renewability, and biodegradability. Several research reports on the use of plant-based inhibitors exist (Umoren et al, 2016; Anadebe et al, 2019; Omotioma et al, 2018; Prabhu et al, 2020), but in each case, determination of optimum parameters was restricted to RSM. It is necessary to test and compare different optimization/prediction tools in corrosion control processes. Thus, this study is aimed at examining the potential of cashew leaf extract for mild steel corrosion mitigation in HCl; with emphasis on comparing RSM and ANN in the performance evaluation.

2.0 Materials and Methodology

2.1 Devices/Equipment

Mild steel, distilled water, HCl, and cashew leaf are among the materials and reagents employed in this investigation. The following tools/devices were used in this investigation: gas chromatography-mass spectrometer and water bath with thermostat. Every chemical utilized in this experiment is of analytical quality.

2.2 Processing of the MS and inhibitor concentration

Samples of uniform sizes (5cm x 4cm x 0.1cm) were cut from the MS sheet. The MS is composed of Ni (0.02), Cr (0.01%), C (0.23%), Mn (0.11%), Si (0.02%), P (0.02%), S (0.02%), Cu (0.01%), and Fe (99.56%). The MS samples were processed through the following steps; degreasing, polishing, cleaning, washing, and drying. For 48 hours, 30.0g of the pulverized cashew leaf was dissolved in 1000 ml of ethanol solvent. Thereafter, the mixture was filtered, and the ethanol in the filtrate was evaporated to produce a concentrated extract. For the study, various dosages of the extract were created. Ten grams of the extract were added to one liter of a stock solution of 1 M HCl. The stock solution was diluted to provide various inhibitory test media (conc.; 0.2 g/L – 1.0 g/L for the corrosion control investigation).

2.3 Characterization of the extract

The cashew leaf extract was subjected to chemical analysis by employing gas chromatography-mass spectrometer – model: GCMS-QP2010 PLUS, SHIMADZU. To classify the various chemical species of the

extract, features of spectrometry and chromatography were jointly considered (Onukwuli and Omotioma, 2019; Odiase-Omoighe and Agoreyo, 2022). When heated in the GC system, the extract was disintegrated into various constituents. An inert aided the movement of the chemical constituents through the system's column. From the GC system, the chemical constituents flew to the spectrophotometer, where the constituents of cashew leaf extract were explicitly identified.

2.4 Gravimetric Method

Previous authors' gravimetric approach was adopted (Omotioma and Onukwuli, 2017; Anadebe et al, 2018; Frolova et al, 2019). Samples of the MS were immersed in the uninhibited and inhibited 1M HCl. In monitoring the weight loss at various times of immersion (t), temperature (T) and inhibitor concentration (C), the ω_t and ω_0 (respective losses in weight in the absence and presence of extract) were measured and used for the evaluation of inhibitor efficiency (\mathcal{E}) and the term of surface coverage (θ). In addition, Langmuir, Frumkin, Temkin, and Flory-Huggins adsorption isotherms of Equations (4), (5), (6), and (7) were employed in the adsorption analyses (Omotioma and Onukwuli, 2017; Onukwuli and Omotioma, 2019). Furthermore, Equation (8) aided the evaluation of the corresponding Gibb's free energy of adsorption (ΔG_{ads}).

$$\theta = \frac{\omega_0 - \omega_1}{\omega_0} \quad (2)$$

$$\mathcal{E} = \frac{\omega_0 - \omega_1}{\omega_0} * 100 \quad (3)$$

$$\log \frac{C}{\theta} = \log C - \log K \quad (4)$$

$$\log \left((C) * \left(\frac{\theta}{1-\theta} \right) \right) = 2.303 \log K + 2\alpha\theta \quad (5)$$

$$\theta = -\frac{2.303 \log K}{2\alpha} - \frac{2.303 \log C}{2\alpha} \quad (6)$$

$$\log \left(\frac{\theta}{C} \right) = \log K + x \log(1 - \theta) \quad (7)$$

$$\Delta G_{ads} = -2.303RT \log(55.5K) \quad (8)$$

where x is the size parameter, R is the gas constant, K is the adsorption equilibrium constant, α is the lateral interaction term, and 'a' is the attractive parameter.

2.4.1 RSM of the optimization process

The experiment was designed on the RSM using the Design-Expert-Software. Following the established technique, the reaction was analyzed using the RSM (Anadebe et al, 2018; Onukwuli and Omotioma, 2016; Amodu et al, 2022). The interactive effects of the parameters on the inhibitor's effectiveness were analyzed using visuals and the Analysis of Variances. The best parameters were found when a mathematical model of the coded factors was developed.

2.4.2 Artificial neural network (ANN)

A three-layered feed-forward neural network was employed on the ANN, with a linear transfer function at the output layer and a tangent sigmoid transfer function at the hidden layer. The efficiency of the inhibitors was anticipated by the proposed model. The back-propagation algorithm was used to train the ANN. MATLAB

R2007b software was used for all computations. Figure 1 displays the ANN architectural analysis. By altering the concealed layer's neuron number, this architecture was controlled. The ANN was simulated using the same experimental dataset that was used for RSM modeling. Three subsets, each with a proportion of about, were created from the entire experimental dataset (20 runs) during the training phase. By dividing the dataset into distinct subsets, it was possible to evaluate the neural network's predictive power to the "hidden" data that was not used for training (Nnanwube and Onukwuli, 2020; Amodu et al, 2022).

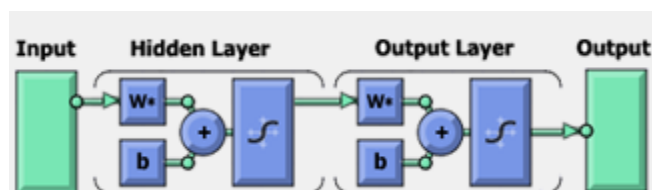


Figure 1: Architectural organ of the ANN analysis

2.4.3 Statistical examination

Previous authors' statistical tools (Nnanwube and Onukwuli, 2020) were employed in the comparative analysis of RSM and ANN efficiencies. Equations (9), (10), and (11) evaluated the coefficient of determination (R^2), root mean square error (RMSE), and standard error of prediction (SEP) respectively.

$$R^2 = 1 - \frac{\sum_{i=1}^n (Y_{exp,i} - Y_{pred,i})^2}{\sum_{i=1}^n (Y_{exp,i} - Y_{pred,ave})^2} \quad (9)$$

$$RMSE = \left(\frac{1}{n} \sum_{i=1}^n (Y_{pred} - Y_{exp})^2 \right)^{1/2} \quad (10)$$

$$SEP = \frac{RMSE}{Y_{exp,ave}} * 100 \quad (11)$$

where n is the sample point number, Y_{pred} is the predicted \mathcal{E} , Y_{exp} is the experimentally determined value \mathcal{E} , $Y_{exp,ave}$ is the experimental average, and Y_{exp} is the experimental value.

3.0 Results and Discussion

3.1 Characteristics of cashew extract

In Figure 2, the GC MS chromatogram of the cashew leaf extract shows various levels of peaks. Each of the peaks represents a chemical constituent. The extract contains 9-tetradecenal, oleic acid, 2-hydroxy cyclopenta decanone, 4H-pyran-4-one, 3,5-dihydroxy-6-methyl-2,3-dihydro-4H-pyran-4-one, 2-methyl-3-ketotetrahydrofuran, oxirane, 8-methyl-9-tetradecenoic acid, 2,3-butylene oxide, 2,3-dimethyloxirane and 3(2H)-furanone. It revealed the presence of chemical compounds of long chain carbon-carbon bond and heteroatoms. Presence of the bio-heterocyclic molecules suggests that cashew leaf extract has corrosion-inhibitive properties (Onukwuli and Omotioma, 2019; Odiase-Omoighe and Agoreyo, 2022).

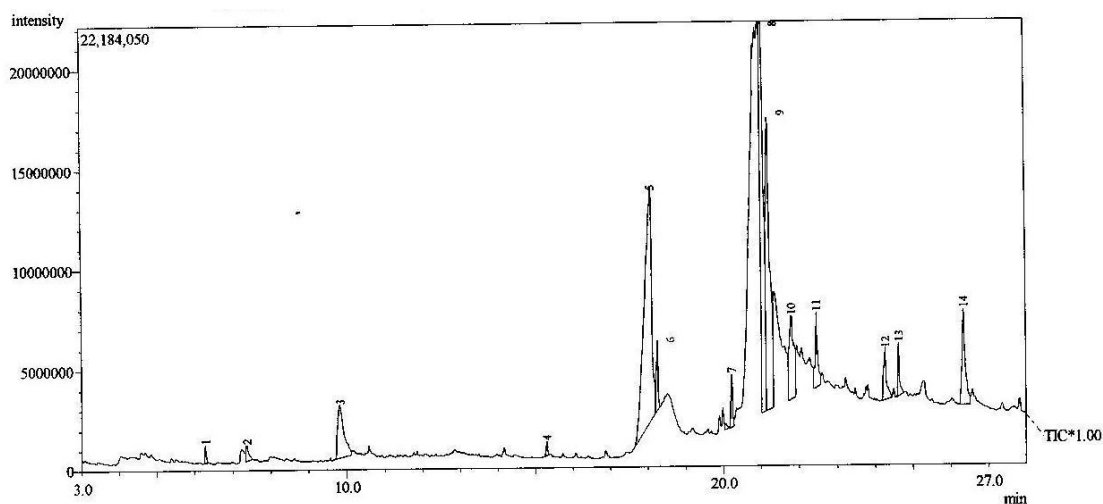


Figure 2: Chromatogram of the cashew leaf extract

3.2 Physical attachment of the inhibitor

Adsorption parameters of the physical attachment process are presented in Table 1. The Frumkin isotherm (FI) is the best-fitting isotherm according to the correlation of determination (R^2) criterion because, in comparison to the Langmuir isotherm (LI), Temkin isotherm (TI), and Flory-Huggins isotherm (FHI), its R^2 values (0.9903 and 0.9845 at 303K and 333K, respectively) are the closest to one (1). An attraction between the molecules of the extract and MS was demonstrated by positive values of the lateral interaction term α (1.9392 and 2.2685 at 303K and 333K, respectively). In each instance, the attractive term (a) is negative; -2.379 and -3.318, 303K and 333K, respectively. It means that the layers of the inhibitor are not interacting. The Gibb's free energy is less than the -40 kJ/mol crucial threshold. Therefore, the inhibitor's adsorption on the MS followed the physical adsorption mechanism. The results concur with the earlier report (Omotioma, and Onukwuli, 2016).

Table 1: Adsorption parameters for the corrosion inhibition

Type	T (K)	R^2	K	ΔG_{ads} (kJ/mol)	α	a	x
LI	303	0.9891	0.7916	-9.5	-	-	-
	333	0.983	0.6236	-9.8	-	-	-
FI	303	0.9903	0.0821	-3.8	1.9392	-	-
	333	0.9845	0.0751	-4.0	2.2685	-	-
TI	303	0.968	40.114	-19.4	-	-2.379	-
	333	0.958	57.651	-22.3	-	-3.318	-
FHI	303	0.931	3.9355	-13.6	-	-	1.106
	333	0.924	4.9203	-15.5	-	-	2.215

3.3 Interactive effects of the variables on the cashew extract's ϵ

Interactive effects of the variables on the efficiency (ϵ) of cashew leaf extract (inhibitor) are displayed in Table 2. Maximum ϵ of 93.94% emerged at an inhibitor concentration of 0.6 g/L, temperature of 318K and time of 16 hrs. The recorded high inhibition efficiency espoused that the extract of cashew is a suitable additive for pickling MS structure. The inhibitive action of the cashew extract could be attributed to the physical attachment

of its components on the surface of the MS. Layer of the adsorbed inhibitor's molecules isolated the MS from the aggressive acid solution (Omotioma et al, 2018).

Table 2: Interactive effects of the factors on the ϵ

Sd.	S/N	Inhibitor conc.(g/L)	T (K)	t (hr)	ϵ (%)
5	1	0.2	303	24	68.56
3	2	0.2	333	8	45.01
14	3	0.6	318	24	88.63
13	4	0.6	318	8	80.59
2	5	1.0	303	8	57.28
10	6	1.0	318	16	80.56
16	7	0.6	318	16	93.94
9	8	0.2	318	16	70.95
12	9	0.6	333	16	78.31
4	10	1.0	333	8	54.55
18	11	0.6	318	16	93.94
15	12	0.6	318	16	93.94
1	13	0.2	303	8	60.65
20	14	0.6	318	16	93.94
19	15	0.6	318	16	93.94
7	16	0.2	333	24	48.81
8	17	1.0	333	24	63.69
11	18	0.6	303	16	84.97
6	19	1.0	303	24	80.75
17	20	0.6	318	16	93.94

3.3.1 Fit summary of the ϵ mathematical model

Table 3 displays a summary of the models' fitness. The optimum mathematical equation describing the inhibition efficiency (ϵ) was found by taking into account four models: linear, 2FI, quadratic, and cubic. The linear and 2FI R^2 values are not closer to one (1). For the cubic model, the adjusted R^2 (0.9911) and the anticipated R^2 (-2.4426) do not reasonably match, the cubic model is not recommended as the best-fitting model. Since the expected R^2 of 0.8930 is near 1 and somewhat consistent with the modified R^2 of 0.9809, the quadratic model is recommended as the best-fitting model. It demonstrates how well the quadratic model can forecast the empirical data.

Table 3: Model's fit summary of the ϵ

Model	Sequential probability	Modified R^2	Expected R^2	
LM	0.4082	0.0038	-0.4974	
2FIM	0.9405	-0.1904	-4.9740	
QM	< 0.0001	0.9809	0.8930	Suggested
CM	0.0686	0.9911	-2.4426	Aliased

LM (linear model), 2FIM (2-factor interaction model), QM (quadratic model), and CM (cubic model).

3.3.2 ANOVA for ϵ quadratic model

Table 4 displays the quadratic model's ANOVA. Fisher test (F-test), degree of freedom (DoF), and probability value were found to be 9, 109.49, and less than 0.0001, respectively. The model appears to be significant based on the F-value of 109.49. The model terms were considered significant if the P-value was less than 0.0500 (Omotioma, and Onukwuli, 2016; Prabhu et al, 2020). The model's sufficient precision of 28.564 suggested that it can be applied to guide the RSM outcome. It agreed with the report of Khaleel et al (2018), where ANOVA was used to establish the significance of quadratic model.

Table 4: ANOVA for the quadratic model of the inhibition efficiency

Basis	SoS	DoF	Mean-square	Fisher-v.	Probability	Sig.
Model	5164.21	9	573.80	109.49	< 0.0001	
A	183.61	1	183.61	35.04	0.0001	
B	382.42	1	382.42	72.97	< 0.0001	
C	274.16	1	274.16	52.31	< 0.0001	
/A*B/	30.42	1	30.42	5.80	0.0367	
/A*C/	54.60	1	54.60	10.42	0.0091	
/B*C/	42.50	1	42.50	8.11	0.0173	
(A) ²	711.10	1	711.10	135.68	< 0.0001	
(B) ²	285.86	1	285.86	54.54	< 0.0001	
(C) ²	143.57	1	143.57	27.39	0.0004	
			R ²		0.9900	
			Modified R ²		0.9809	
			Expected R ²		0.8930	
			Adequate Precision		28.5643	

SoS (Sum of Squares), A (inh. conc.), B (temp.), C (time).

3.3.3 The Mathematical model

Equations 1 and 2 present mathematical models of the extract's efficacy (E) for the coded and real variables, respectively. Since two (2) is the maximum power of the variables, all of the equations are quadratic. The model's positive indicators suggested a synergistic impact, whilst its negative indicators suggested an antagonistic effect. The coded equation forecasts how the dependent variable will react at the designated levels (Odejobi and Akinbulumo, 2019; Anadebe et al, 2019; Omotioma et al, 2018). By comparing the factor coefficients, the resulting coded equation can be used to determine the relative importance of the factors.

$$E = + 93.10 + 4.28A - 6.18B + 5.24C + 1.95AB + 2.61AC - 2.30BC - 16.08A^2 - 10.20B^2 - 7.23C^2 \tag{12}$$

$$E = - 4467.91295 + 14.90341\text{Inhibitor conc.} + 28.51922\text{Temp.} + 9.88563\text{Time} + 0.325000\text{Inhibitor conc.} * \text{Temp.} + 0.816406\text{Inhibitor conc.} * \text{Time} - 0.019208\text{Temp.} * \text{Time} - 100.50284\text{Inhibitor conc.}^2 - 0.045313\text{Temp.}^2 - 0.112898\text{Time}^2 \tag{13}$$

3.3.4 Graphics of the RSM result

Figure 3 shows the RSM's graphic imagery. A linear graph comparing predicted and actual inhibition efficiency (E) was displayed. The dots clustered along the line of best fit, signifying that the experimental data was sufficiently explained by the generated model. The E rose as concentration increased on the 3-D image until it reached the apex. The interaction impact of time on E showed a similar pattern. But as the temperature rose, the value of E fell. Furthermore, a peak displaying optimal/predicted E was revealed. These findings are consistent with those of earlier studies (Anadebe et al, 2018; Amodu et al, 2022).

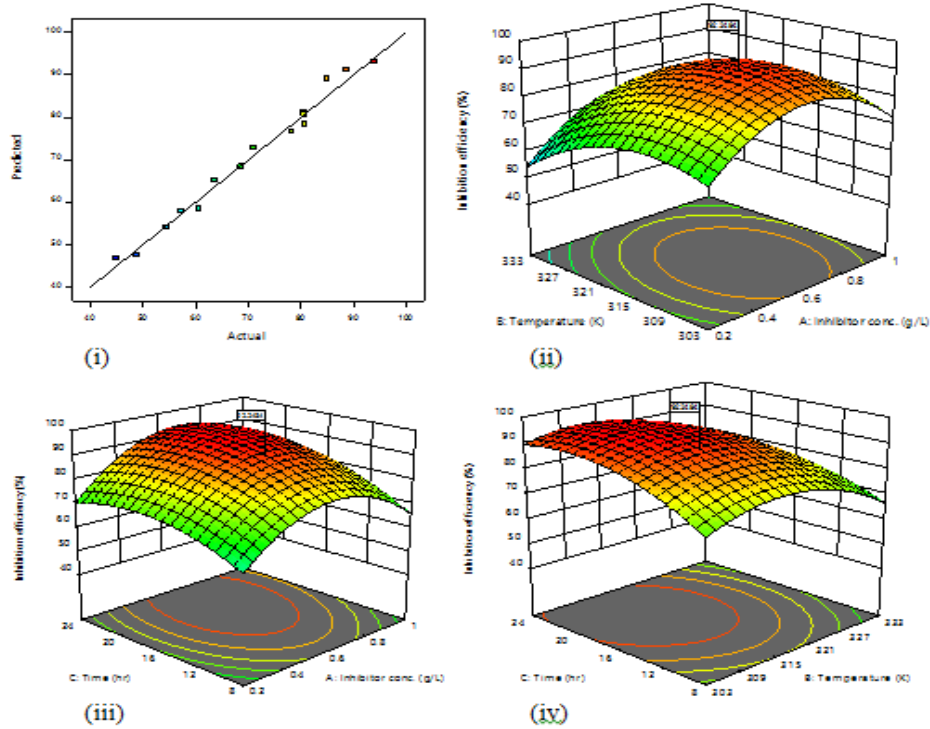


Figure 3: The \mathcal{E} of cashew leaf extract

(i) Predicted against actual \mathcal{E} , (ii) \mathcal{E} against conc. and temp., (iii) \mathcal{E} versus conc. and time, (iv) \mathcal{E} against temp. and time.

3.4 Artificial Neural Network (ANN) Analysis

Figures 4 and 5 display the respective performance and regressional analyses of the ANN used for the prediction of the cashew leaf's IE. The trained network's performance plot showed seven epochs, indicating that the ANN is capable of accurately forecasting the cashew leaf's ideal IE. The prediction ability of the ANN is in line with the report of Millán-Ocampo et al (2018). Training outputs against targets, validation outputs against targets, and test outputs against targets were the three graphs that were shown. The output and the target data have a strong association, as demonstrated by the linear graphs they displayed.

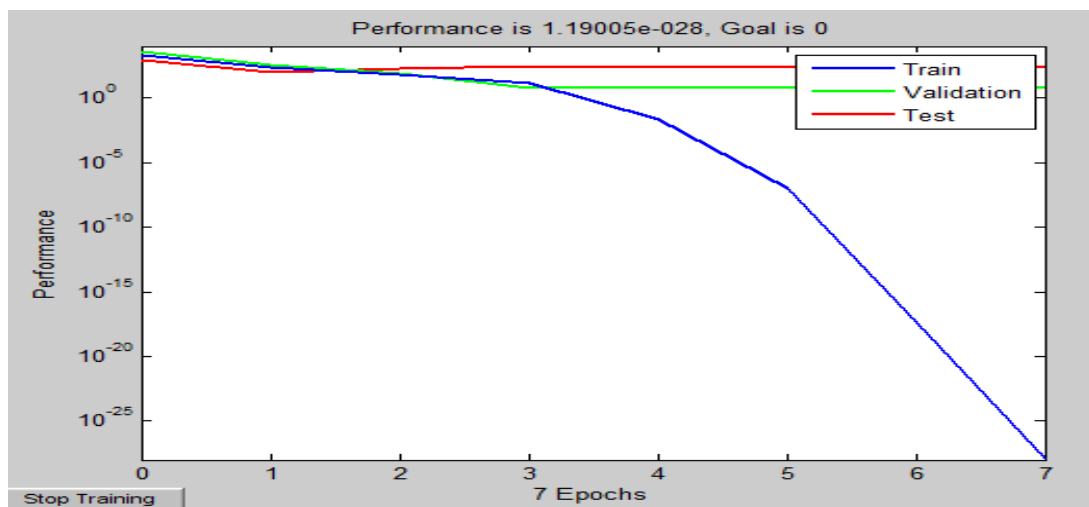


Figure 4: Performance network

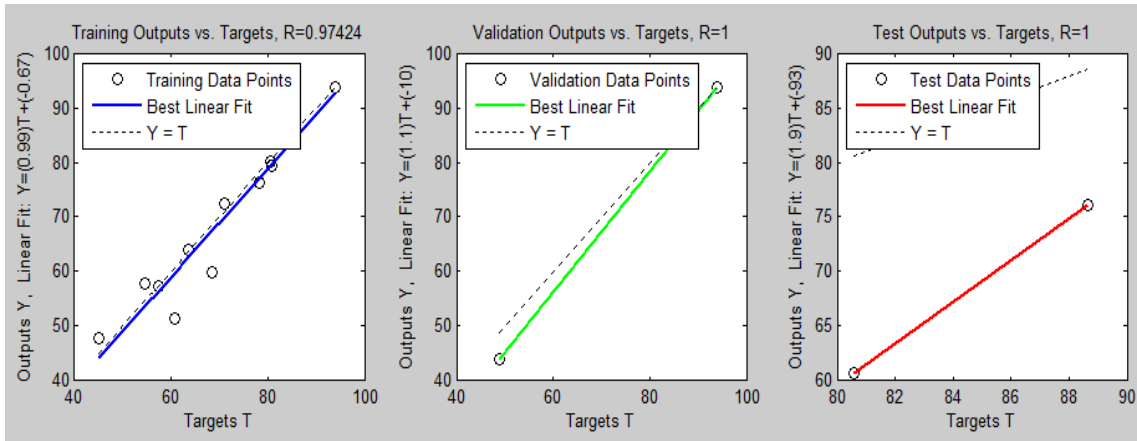


Figure 5: Regression network

3.5 Comparison of the RSM and ANN

The inhibitory efficiency (ϵ) comparison between RSM and ANN results is shown in Table 5. It displayed both the expected/optimal values of the inhibition efficiencies and the actual experimental outcomes of the 20-run experimental design. To evaluate the ANN and RSM's relative estimate and prediction capabilities, a comparison analysis was conducted using a number of statistical metrics. Table 6 displays the statistical analyses. The ANN gave high R^2 of 0.971309, compared to that of RSM, 0.96389, suggesting the superiority of ANN over RSM for predictability of ϵ . Also, ANN gave a better prediction than RSM because the values of RMSE and SEP were lower than those of RSM. It corroborates the findings revealed by the R^2 values, which are in line with the previous reports (Nnanwube and Onukwuli, 2020; Amodu et al, 2022). The goodness of fit of the model was established by the statistical outcome.

Table 5: Comparison of ϵ of RSM and ANN predicted Results

Sd.	S/N	Inh. conc. g/L	T K	T hr	Actual ϵ %	RSM predicted ϵ %	ANN predicted ϵ %
5	1	0.2	303	24	68.56	68.37	67.2
3	2	0.2	333	8	45.01	46.86	43.89
14	3	0.6	318	24	88.63	91.11	87.07
13	4	0.6	318	8	80.59	80.64	79.11
2	5	1.0	303	8	57.28	57.96	56.04
10	6	1.0	318	16	80.56	81.30	79.08
16	7	0.6	318	16	93.94	93.10	92.33
9	8	0.2	318	16	70.95	72.73	69.57
12	9	0.6	333	16	78.31	76.72	76.86
4	10	1.0	333	8	54.55	54.10	53.33
18	11	0.6	318	16	93.94	93.10	92.33
15	12	0.6	318	16	93.94	93.10	92.33
1	13	0.2	303	8	60.65	58.52	59.37
20	14	0.6	318	16	93.94	93.10	92.33
19	15	0.6	318	16	93.94	93.10	92.33
7	16	0.2	333	24	48.81	47.50	47.65
8	17	1.0	333	24	63.69	65.19	62.38
11	18	0.6	303	16	84.97	89.09	83.45
6	19	1.0	303	24	80.75	78.27	79.27
17	20	0.6	318	16	93.94	93.10	92.33

Table 6: Statistics of the predictions

Property	RSM	ANN
RMSE	1.618362	1.442544
R ²	0.96389	0.971309
SEP	2.119731	1.889445

Conclusion

The study focused on the potential of cashew leaf extract for mild steel corrosion mitigation in hydrochloric acid environment. In the experimental investigation, adsorption mechanism and characteristics of the corrosion inhibition process were successfully determined using the gravimetric procedure. It involved the comparison of RSM and ANN in the performance evaluation of the cashew leaf as corrosion inhibitor. Biomolecules of 9-tetradecenal, oleic acid, 2-hydroxy cyclopenta decanone, 4H-pyran-4-one, 3,5-dihydroxy-6-methyl-2,3-dihydro-4H-pyran-4-one, oxirane, 8-methyl-9-tetradecenoic acid, 2,3-butylene oxide, 2,3-dimethyloxirane, 2-methyl-3-ketotetrahydrofuran and 3(2H)-furanone were among the results of the analysis. The cashew leaf extract's molecular species spontaneously adhered to the MS by physical adsorption. At 318K, 16 hours, and a C of 0.6 g/L, the highest ϵ of 93.94% was achieved. The high ϵ value indicated that cashew extract is a good addition to MS pickling. In terms of forecasting the cashew extract's efficacy on the prediction tools, ANN outperformed RSM. Recorded optimum parameters of this study are significant, and they provided suitable criteria for deploying plant extract in corrosion mitigation process.

References

- Amodu, O.S., Odunlami, M.O., Akintola, J.T., Ojumu, T.V. and Ayanda, O.S., 2022. Artificial neural network and response surface methodology for optimization of corrosion inhibition of mild steel in 1 M HCl by *Musa paradisiaca* peel extract. *Heliyon*, 8(12).
- Anadebe, V.C., Onukwuli, O.D., Omotioma, M. and Okafor, N.A., 2019. Experimental, theoretical modeling and optimization of inhibition efficiency of pigeon pea leaf extract as anti-corrosion agent of mild steel in acid environment. *Materials Chemistry and Physics*, 233, pp.120-132.
- Anadebe, V.C., Onukwuli, O.D., Omotioma, M. and Okafor, N.A., 2018. Optimization and electrochemical study on the control of mild steel corrosion in hydrochloric acid solution with bitter kola leaf extract as inhibitor. *South African Journal of Chemistry*, 71, pp.51-61.
- Bell, S., Steinberg, T. and Will, G., 2019. Corrosion mechanisms in molten salt thermal energy storage for concentrating solar power. *Renewable and Sustainable Energy Reviews*, 114, p.109328.
- Frolova, L.V., Kashkovsky, R.V. and Sayapin, A.O., 2019. Gravimetric and electrochemical testing of multipurpose corrosion inhibitors with biocidal action. *International Journal of Corrosion and Scale Inhibition*, 8(3), pp.529-538.
- Kadhim, A., Betti, N., Al-Bahrani, H.A., Al-Ghezi, M.K.S., Gaaz, T., Kadhum, A.H. and Alamiery, A., 2021. A mini review on corrosion, inhibitors and mechanism types of mild steel inhibition in an acidic environment. *International Journal of Corrosion and Scale Inhibition*, 10(3), pp.861-884.
- Khaleel, H., Ateeq, A.A. and Ali, A.A., 2018. The effect of temperature and inhibitor on corrosion of carbon steel in acid solution under static study. *Int. J. Appl. Eng. Res*, 13(6), pp.3638-3647.
- Mashuga, M.E., Olasunkanmi, L.O. and Ebenso, E.E., 2017. Experimental and theoretical investigation of the inhibitory effect of new pyridazine derivatives for the corrosion of mild steel in 1 M HCl. *Journal of Molecular Structure*, 1136, pp.127-139.
- Millán-Ocampo, D.E., Parrales-Bahena, A., González-Rodríguez, J.G., Silva-Martínez, S., Porcayo-Calderón, J. and Hernández-Pérez, J.A., 2018. Modelling of behavior for inhibition corrosion of bronze using artificial neural network (ANN). *Entropy*, 20(6), p.409.

- Nnanwube, I.A. and Onukwuli, O.D., 2020. Modelling and optimization of zinc recovery from Enyigba sphalerite in a binary solution of hydrochloric acid and hydrogen peroxide. *Journal of the Southern African Institute of Mining and Metallurgy*, 120(11), pp.609-616.
- Odejobi O., J. and Akinbulumo O., A., 2019. Modeling and optimization of the inhibition efficiency of Euphorbia heterophylla extracts based corrosion inhibitor of mild steel corrosion in HCl media using a response surface methodology. *Journal of Chemical Technology and Metallurgy*, 54(1), pp.217-232.
- Odiase-Omoighe, J.O. and Agoreyo, B.O., 2022. Identification of Bioactive Compounds in Sclerotia Extracts from Pleurotus tuber-regium (Fr.) Sing. using Gas Chromatograph–Mass Spectrometer (GC-MS). *Nigerian Journal of Biotechnology*, 38(1), pp.39-50.
- Omotioma, M. and Onukwuli, O.D., 2016. Modeling the corrosion inhibition of mild steel in HCl medium with the inhibitor of pawpaw leaves extract. *Portugaliae Electrochimica Acta*, 34(4), pp.287-294.
- Omotioma, M. and Onukwuli, O.D., 2017. Evaluation of pawpaw leaves extract as anti-corrosion agent for aluminium in hydrochloric acid medium. *Nigerian Journal of Technology*, 36(2), pp.496-504.
- Omotioma, M., Onukwuli, O.D. and Obiora-Okafo, I., 2019. Phytochemicals and inhibitive properties of Cashew extract as corrosion inhibitor of aluminium in H₂SO₄ medium. *Latin American Applied Research*, 49, pp.99-103.
- Onukwuli and Omotioma, 2016. Optimization of the inhibition efficiency of mango extract as corrosion inhibitor of mild steel in 1.0M H₂SO₄ using response surface methodology. *Journal of Chemical Technology & Metallurgy*, 51(3).
- Onukwuli, O.D. and Omotioma, M., 2019. Study of bitter leaves extract as inhibitive agent in HCl medium for the treatment of mild steel through pickling. *Portugaliae Electrochimica Acta*, 37(2), pp.115-121.
- Prabhu, P.R., Prabhu, D. and Rao, P., 2020. Analysis of Garcinia indica Choisy extract as eco-friendly corrosion inhibitor for aluminum in phosphoric acid using the design of experiment. *Journal of Materials Research and Technology*, 9(3), pp.3622-3631.
- Rodriguez-Clemente, E., Barrera-Pascual, V., Cervantes-Cuevas, H., Aldana-González, J., Uruchurtu-Chavarin, J., Romero-Romo, M. and Palomar-Pardavé, M., 2018. New 1-(2-pyridinyl)-2-(o-, m-, p-hydroxyphenyl) benzimidazoles as corrosion inhibitors for API 5L X52 steel in acid media. *Anti-Corrosion Methods and Materials*, 65(2), pp.166-175.
- Salleh, S.Z., Yusoff, A.H., Zakaria, S.K., Taib, M.A.A., Seman, A.A., Masri, M.N., Mohamad, M., Mamat, S., Sobri, S.A., Ali, A. and Ter Teo, P., 2021. Plant extracts as green corrosion inhibitor for ferrous metal alloys: A review. *Journal of Cleaner Production*, 304, p.127030.
- Umoren, S.A., Eduok, U.M., Solomon, M.M. and Udoh, A.P., 2016. Corrosion inhibition by leaves and stem extracts of Sida acuta for mild steel in 1 M H₂SO₄ solutions investigated by chemical and spectroscopic techniques. *Arabian journal of chemistry*, 9, pp.S209-S224.
- Ushakov, I. A., Nikonova, V. S., Polynskii, I. V., Knyazeva, L. G., Polynskaya, M. M., & Antsiferov, E. A. (2021). Study on Efficiency of Corrosion Inhibitors Based on Derivatives of Isothiuronic Salts. *Proceedings of Universities. Applied Chemistry and Biotechnology*, 11 (2), pp.326-332. <https://doi.org/10.21285/2227-2925-2021-11-2-326-332>.
- Xia, D.H., Deng, C.M., Macdonald, D., Jamali, S., Mills, D., Luo, J.L., Strebl, M.G., Amiri, M., Jin, W., Song, S. and Hu, W., 2022. Electrochemical measurements used for assessment of corrosion and protection of metallic materials in the field: A critical review. *Journal of Materials Science & Technology*, 112, pp.151-183.
- Yadav, M., Gope, L., Kumari, N. and Yadav, P., 2016. Corrosion inhibition performance of pyranopyrazole derivatives for mild steel in HCl solution: gravimetric, electrochemical and DFT studies. *Journal of Molecular Liquids*, 216, pp.78-86.